

Supplementary Information

Tuning selectivity and activity of Au catalysts for carbon dioxide electroreduction via grain boundary engineering: a DFT study

Cunku Dong,^{a,b} Jianyu Fu,^a Hui Liu,^a Tao Ling,^a Jing Yang,^a Shi Zhang, Qiao^{a,c,*} and
Xi-Wen Du^{a,*}

^aInstitute of New Energy Materials, School of Materials Science and Engineering,
Tianjin University, Tianjin 300072, People's Republic of China

^bKey Laboratory of Advanced Ceramics and Machining Technology, Ministry of
Education, Tianjin University, Tianjin, 300072, People's Republic of China

^cSchool of Chemical Engineering, University of Adelaide, Adelaide, SA 5005,
Australia

AUTHOR INFORMATION

Corresponding Author

*xwdu@tju.edu.cn and s.qiao@adelaide.edu.au

Computational details

1. AuGBS and Flat Surface Models. Au bulks containing grain boundary (AuGB) were modeled according to coincidence site lattice (CSL) theory,^{1,2} as described by the following expression,

$$\Sigma = X^2 + NY^2 \quad (1)$$

$$\theta = 2\arctan\left(\frac{Y}{X\sqrt{N}}\right) \quad (2)$$

$$N = h^2 + k^2 + l^2 \quad (3)$$

where Σ specifies the relation between the two grains unambiguously; $1/\Sigma$ is the proportion of coincidence sites in the crystal lattice. θ indicates the rotation angle for a given facet (hkl) around the rotation axis $[hkl]$ to make sure that $1/\Sigma$ of lattice sites is coincided in an elementary periodic supercell. N denotes the sum of the squares of the indices of a crystal facet (h , k and l); X and Y are two prime numbers with no common factor. As such, two GB bulk models with low-index (100) and (110) facets were built considering the compromise between computational cost and accuracy, denoted as Au $\Sigma 5\{021\}/[100]$ GB and Au $\Sigma 6\{2-21\}/[110]$ GB. Low-index AuGB surface (GBS) was constructed *via* exposing the corresponding low-index planes such as (100) plane and (110), denoted as Au(100)GBS and Au(110)GBS, respectively. To model low-index extended Au(100) and Au(110), and Au(111) flat surfaces (Figure S1), we used an elementary surface GB supercell with three-layer slab on the basis of the optimized lattice constants of Au bulk ($a=b=c=4.22$ Å). For structural relaxation and electronic calculation, adsorbate and the uppermost layer were allowed to fully relax in all configurations, while the rest layers were kept fixed during the course of relaxation. A

vacuum space of 15 Å perpendicular to the slab surface was used to avoid artificial interactions due to the periodicity boundary condition.

2. Computational Details. All periodic density functional theory (DFT) calculations in this study were performed using Vienna ab initio simulation program (VASP), a plane-wave DFT software package.^{3,4} The exchange-correlation interactions were modeled by revised Perdew-Burke-Ernzerhof (rPBE)^{5,6} functional within the generalized gradient approximation (GGA) implemented with the projector-augmented-wave (PAW) function method⁷ for representing the nonvalence core electrons. Spin-polarization was considered in all calculations except free gaseous species. A plane-wave cutoff energy was set as 450 eV. 0.1 eV of Fermi-level smearing was used for all geometrical relaxation, including bulk, adsorbate-surface and gas-phase species. The relaxation for these systems was completed when the maximum force exerted on each atom is less than 0.05 eV/Å. The adsorption of intermediates at the atop sites is considered for various catalysts throughout our work. The perfect Au bulk was fully optimized using $16 \times 16 \times 16$ k-point Monkhorst–Pack mesh sampling. For Au slab calculations, $2 \times 1 \times 1$ k-point Monkhorst–Pack mesh sampling was employed for AuGBS and GB-free surface in the surface Brillouin zone.

Gibbs free energies (G) for each gaseous and adsorbed species were calculated at 298.15 K and 101325 Pa, according to the following expression:

$$G = E_{DFT} + E_{ZPE} + \int C_p dT - TS \quad (4)$$

where E_{DFT} is the electronic energy calculated with VASP; E_{ZPE} is the zero-point energy; $\int C_p dT$ is the enthalpic temperature correction; $-TS$ is the entropy contribution to G .

As previously described, standard ideal gas method was used to calculate E_{ZPE} , $\int C_p dT$ and $-TS$ from temperature, pressure, and calculated vibrational energies.⁸ Free energies of each adsorbate on the surfaces were calculated by treating all $3N$ degrees of freedom of the adsorbate as frustrated harmonic vibrations given that the contribution from the vibrations of the substrate is negligible. All vibrations were treated in the harmonic oscillator approximation.

The computational hydrogen electrode (CHE) model was employed to determine free energies of reaction intermediates under an applied external potential (U).⁹ In the CHE model, each electrochemical reaction step occurring at a catalyst surface involves a simultaneous proton-electron pair transfer. The chemical potential of a proton-electron pair, $\mu[H^+ + e^-]$, is equal to a half of the chemical potential of gaseous hydrogen at $U=0$ vs the reversible hydrogen electrode (RHE), 101325 Pa of H_2 , 298.15 K, and all pH values, $\mu[H^+ + e^-] = 0.5\mu[H_2]$. When the external bias voltage U is applied, the chemical potential of the proton-electron pair is shifted by $-eU$, that is $\mu[H^+ + e^-] = 0.5\mu[H_2] - eU$.

\overline{CN} of active site i on the surface is estimated:

$$\overline{CN}(i) = \sum_{j=1}^{n_i} \frac{cn(j)}{cn_{max}} \quad (5)$$

where $cn(j)$ indicates each first-nearest neighbor atom j with its own coordination number, while cn_{max} is referred to as the maximum number of first-nearest neighbors in the bulk ($cn_{max}=12$ for an face-centered cubic crystal). The sum spans all of the first-nearest neighbors (n_i).

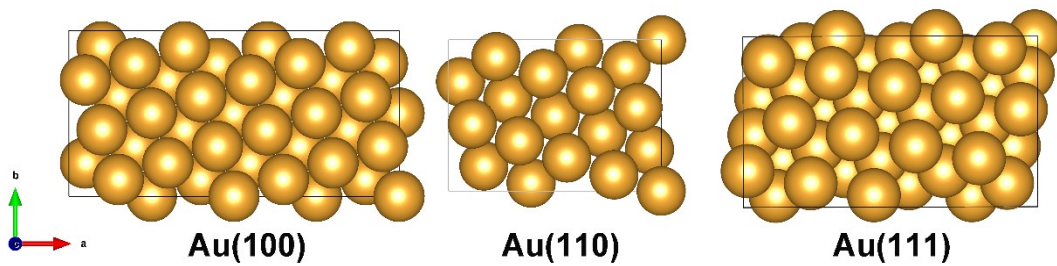


Figure S1. Top views of fully relaxed periodic supercells for flat Au(100), Au(110) and Au(111) surface.

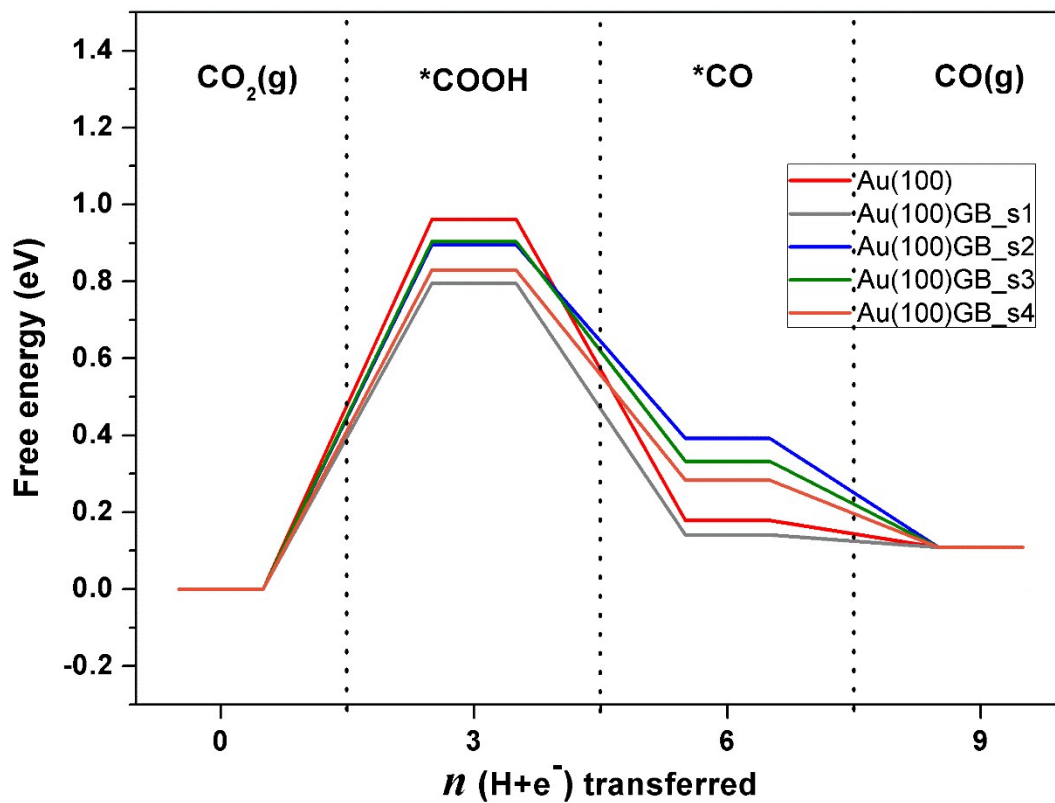


Figure S2. Free energy diagrams for electrochemical reduction reaction of CO_2 to CO at zero electrode potential ($U = 0$ V) on site 1-4 at Au(100)GBS and flat Au surface. n indicates the number of proton-electron pair transfer during CO_2RR .

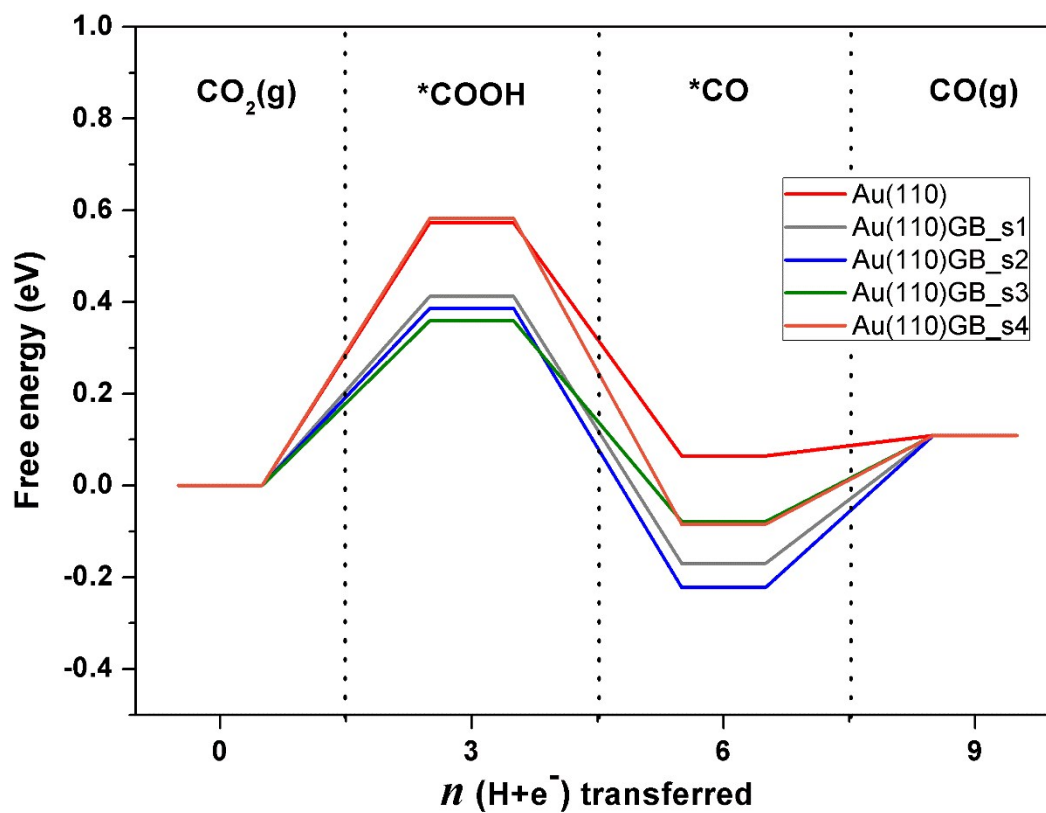


Figure S3. Free energy diagrams for electrochemical reduction reaction of CO₂ to CO at zero electrode potential ($U = 0$ V) on site 1-4 at Au(110)GBS and flat Au surface. n indicates the number of proton-electron pair transfer during CO₂RR.

Table S1. Calculated values for the zero-point energy correction, enthalpy correction, and entropy correction to free energies of free gaseous species. Assumed fugacities for gaseous species are also included.

Species	Fugacity (Pa)	E_{ZPE} (eV)	$\int C_p dT$ (eV)	$-TS$ (eV)	$G-E_{\text{elec}}$ (eV)
CO ₂ (gas)	101325	0.31	0.10	-0.66	-0.26
CO (gas)	101325	0.13	0.09	-0.61	-0.39
H ₂ (gas)	101325	0.27	0.09	-0.42	-0.06
H ₂ O (gas)	3534	0.58	0.10	-0.65	0.03
CH ₄ (gas)	20467	1.20	0.10	-0.60	0.70
CH ₃ OH (gas)	6079	1.35	0.11	-0.79	0.67

Table S2. Calculated values for the zero-point energy correction, enthalpy correction, and entropy correction to free energies of adsorbed COOH, CO and H on Au(111), Au(100) and Au(110) surface, respectively.

Species	E_{ZPE} (eV)	$\int C_p dT$ (eV)	$-TS$ (eV)	$G-E_{\text{elec}}$ (eV)
*COOH@Au(111)	0.61	0.11	-0.23	0.49
*CO@Au(111)	0.18	0.08	-0.18	0.08
*H@Au(111)	0.15	0.03	-0.05	0.14
*COOH@Au(100)	0.61	0.11	-0.19	0.52
*CO@Au(100)	0.18	0.08	-0.18	0.08
H@Au(100)	0.1470	0.03	-0.06	0.12
*COOH@Au(110)	0.61	0.11	-0.27	0.45
*CO@Au(110)	0.18	0.09	-0.20	0.07
*H@Au(110)	0.1443	0.03	-0.07	0.10

Table S3. Calculated values for the zero-point energy correction, enthalpy correction, and entropy correction to free energies of adsorbed COOH, CO, CHO and H on Au(100)GBS and Au(110)GBS, respectively.

Species	E_{ZPE} (eV)	$\int C_p dT$ (eV)	$-TS$ (eV)	$G-E_{\text{elec}}$ (eV)
*COOH@Au(100)GBS_s1	0.60	0.11	-0.2055	0.5129
*COOH@Au(100)GBS_s2	0.61	0.11	-0.2423	0.4764
*COOH@Au(100)GBS_s3	0.61	0.11	-0.2422	0.4764
*COOH@Au(100)GBS_s4	0.61	0.11	-0.2669	0.4517
*COOH@Au(110)GBS_s1	0.61	0.11	-0.2146	0.5033
*COOH@Au(110)GBS_s2	0.61	0.11	-0.2377	0.4806
*COOH@Au(110)GBS_s3	0.61	0.11	-0.2340	0.4852
*COOH@Au(110)GBS_s4	0.61	0.11	-0.2401	0.4775
*CO@Au(100)GBS_s1	0.18	0.08	-0.19	0.07
*CO@Au(100)GBS_s2	0.17	0.09	-0.20	0.07
*CO@Au(100)GBS_s3	0.17	0.09	-0.22	0.04
*CO@Au(100)GBS_s4	0.18	0.09	-0.19	0.07
*CO@Au(110)GBS_s1	0.19	0.08	-0.17	0.10
*CO@Au(110)GBS_s2	0.19	0.08	-0.18	0.08
*CO@Au(110)GBS_s3	0.18	0.08	-0.17	0.10
*CO@Au(110)GBS_s4	0.17	0.09	-0.19	0.07
*CHO@Au(110)GBS_s1	0.46	0.08	-0.19	0.36
*CHO@Au(110)GBS_s2	0.46	0.09	-0.19	0.36
*CHO@Au(110)GBS_s3	0.46	0.08	-0.18	0.36
*CHO@Au(110)GBS_s4	0.46	0.09	-0.19	0.36
*H@Au(100)GBS_s1	0.14	0.04	-0.08	0.10
*H@Au(110)GBS_s1	0.15	0.03	-0.05	0.13

Table S4 Calculated values for the zero-point energy correction, enthalpy correction, and entropy correction to free energies of adsorbed CH₂O, CH₃ and O on Au(110)GBS, respectively.

Species	E_{ZPE} (eV)	$\int C_p dT$ (eV)	$-TS$ (eV)	$G-E_{elec}$ (eV)
*CH ₂ O@Au(110)GBS_s1	0.72	0.13	-0.31	0.54
*CH ₃ O@Au(110)GBS_s1	1.07	0.11	-0.22	0.96
*O@Au(110)GBS_s(1)	0.05	0.04	-0.09	0.01
*CH ₂ O@Au(110)GBS_s2	0.74	0.11	-0.25	0.60
*CH ₃ O@Au(110)GBS_s2	1.07	0.10	-0.21	0.97
*O@Au(110)GBS_s(2)	0.05	0.04	-0.09	0.01
*CH ₃ O@Au(110)GBS_s3	1.06	0.11	-0.27	0.90
*O@Au(110)GBS_s(3)	0.05	0.04	-0.09	0.01
*CH ₃ O@Au(110)GBS_s4	1.07	0.10	-0.21	0.96
*O@Au(110)GBS_s(4)	0.05	0.04	-0.09	0.01

Reference

- (1) Sutton, A.P.; Balluffi R.W. Interfaces in crystalline materials. **1995**, Oxford: Oxford Scientific Publications.
- (2) Hart E. W. The nature and behavior of grain boundaries. **1972**. New York: Plenum; p. 155.
- (3) Kresse, G.; Joubert, D. Phys. Rev. B: Condens. Matter Mater. Phys. **1999**, 59, 1758.
- (4) Kresse, G.; Furthmüller, J. *Comput. Mater. Sci.* **1996**, 6, 15–50.
- (5) Perdew, J. P.; Burke, K.; Ernzerhof, M. *Phys. Rev. Lett.* **1996**, 77, 3865.
- (6) Hammer, B.; Hansen, L. B.; Nørskov, J. K. *Phys. Rev. B: Condens. Matter Mater. Phys.* **1999**, 59, 7413.
- (7) Blöchl, P. E. Phys. Rev. B: Condens. Matter Mater. Phys. **1994**, 50, 17953.
- (8) Cramer, C. J. Essentials of Computational Chemistry Theories and Models; 2004; Vol. 42, pp. 334–342.

(9) Nørskov, J. K.; Rossmeisl, J.; Logadottir, A.; Lindqvist, L.; Kitchin, J. R.; Bligaard, T.; Jonsson, H. *J. Phys. Chem. B* **2004**, *108*, 17886-17892.